

# Large-Scale Sediment Inflow and Bed-Variation from 12th Typhoon (2011) in the Asahi River Basin

Y. Tsukamoto

*Graduate School of Science and Engineering, Chuo University, Japan*

T. Eguchi

*The Kansai Electric Power Co., Japan*

S. Fukuoka

*Research and Development Initiative, Chuo University, Japan*

**ABSTRACT:** In the Asahi River, heavy rainfall from 12th typhoon (2011) had caused the river channel blockade by sediment inflow due to slope failures and debris flows. These phenomena make large amount of sediment discharge into the river shortly, and change the river channel characteristics, such as the channel shapes, and grain size distributions. So, it is important to clarify the mechanism of sediment transports including large amount of sediment supply for the river management. In this study, first, we clarified points of slope failures and characteristic changes in river channel by large-scale sediment inflow using observed data and aerial photographs. In order to estimate the volume of sediment inflow, numerical analysis of slope failures and debris flows were made. Furthermore, we combined two-dimensional flood flow model with river bed variation model and examined the sediment transport mechanism including the sediment supply in the Asahi River during the 2011 flood.

*Keywords: Sediment inflow, Sediment transport, Debris flow, Slope failure, Numerical model, Stony-bed river, Bed variation, Grain size distribution*

## 1 INTRODUCTION

A heavy rainfall from 12th typhoon (2011) brought large-scale floods and slope failures in the Asahi River basin. Sediment supply to the Asahi River due to slope failures changed channel shapes and grain size distributions of the river bed remarkably in the short period of time. Estimation of the amount of the sediment supply of debris flows by slope failures and understanding of sediment transports during the flood are important for the river management.

The Asahi River is a stony-bed river with a wide range of grain-size distributions. In the Asahi River, a sediment bypass tunnel is installed for a measure against turbid water of a dam reservoir, and the reservoir sedimentation. Fukuda et al. (2012) investigated the recovery mechanism of riffles and pools and flushing mechanism of reservoir sedimentation by using the two-dimensional flood flows and bed variation analysis in stony-bed river (Osada et al. (2013)). However, sediment inflows from mountain streams were not considered in this model, because the flood discharge was relatively small compared with the 2011 flood.

The slope failures and debris flow simulation model to estimate sediment inflows from mountain streams has been proposed by researchers. For example, there are physically-based model of the SHETRAN (Bathust (2002)) and the SERMOW- II (Hirasawa et al. (2012)) and so on. Ichikawa (1999) calculated the sediment runoff due to slope failures using by the kinematic wave-runoff model and slope failure model considering an infinite length slope-stability analysis. And sediment inflows from mountain streams were simulated by using debris flow equations which corresponded to each regime such as debris flow, immature debris flow, and bed load (Takahashi (2001)). But, these researches have not considered enough the relation between flood flows and large-scale sediment inflow, and applicability to the design of structures for sedimentation. Therefore, it is important to clarify mutual relations of sediment transports in river channel, mountain stream, dam reservoir and outlet structure.

The objectives of this study are to clarify the sediment transport mechanism based on observed data and to develop the two-dimensional flood flows and river bed variation analysis model clarifying the

relationship between flood flows and sediment transports including the large amount of sediment supply of debris flows.

## 2 SEDIMENT YIELD AND RIVER CHANNEL CHANGE

### 2.1 Characteristics of the Asahi River basin

Figure 1 shows the plan form of the Asahi River basin and the flushing bypass tunnel. The Asahi River is a stony-bed river with a wide range of grain-size distributions. The channel shapes are remarkably meandering, and the river bed gradients of upstream and downstream in Asahi Dam is about 1:80 and 1:100, respectively.

Asahi Dam is located at about 6.0km point of the Asahi River from the junction with the Kumano River. The sediment flushing bypass tunnel indicated by the red line in Figure 1 was constructed to mitigate the long-term turbid water and reservoir sedimentations in Asahi Dam Reservoir. The sediment flushing bypass tunnel is a 2,350m long, and 1:35 bed gradient.

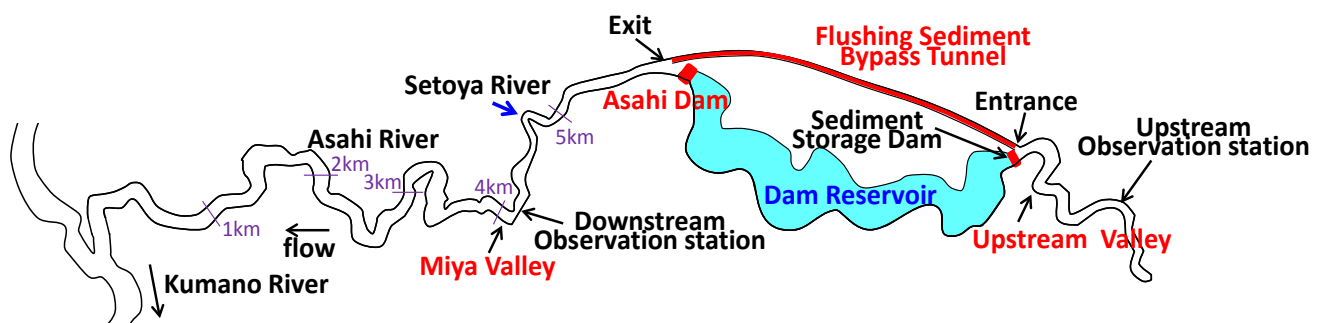


Figure 1. Plan form of the Asahi River basin.

### 2.2 Objective flood

Figure 2 shows the rainfall heightgraph, the water level hydrograph, inflow and outflow discharge hydrographs in Asahi Dam Reservoir observed by the 12th typhoon (2011). The flood had three peaks and recorded the largest rainfall of totals about 1,500mm for three days.

Figure 3 shows the observed discharge hydrographs in upstream and downstream observation station. The observed discharge hydrograph in upstream observation station was 708 m<sup>3</sup>/s, and in downstream observation station was 685 m<sup>3</sup>/s. The maximum annual discharge in upstream observation station was 219 m<sup>3</sup>/s and in downstream observation station was 244 m<sup>3</sup>/s. Hence, the flood was a large flood comparable to three times of the annual maximum discharge.

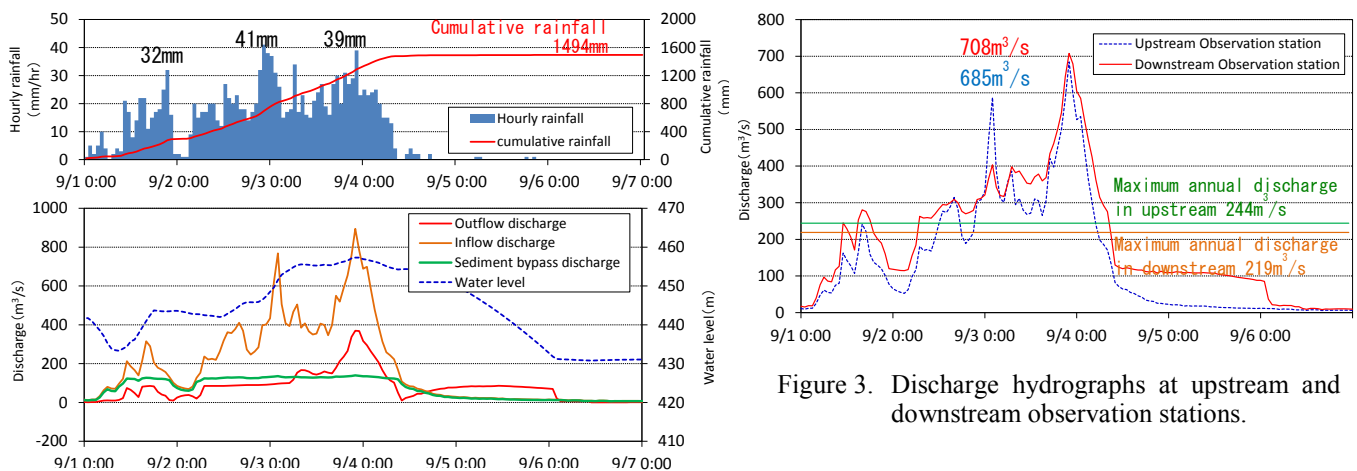


Figure 3. Discharge hydrographs at upstream and downstream observation stations.

Figure 2. Heiehtgraph and hydrographs in the Dam Reservoir.

### 2.3 Sediment yield and river channel change

Figure 4 shows comparison between aerial photographs before and after the flood in the slope failure point and the exit of the Miya Valley. The aerial photographs were taken after (September 2011 by Geographical Information Authority of Japan) and before (May 2004 by Ministry of Agriculture, Forestry and Fisheries of Japan) the flood. The investigation of slope failures points in the Asahi River basin showed the large-scale slope failure (about 82,000 m<sup>2</sup>) at the Miya Valley (see figure 4 (a)).

Figure 4 (b) shows river channel change at the exit of mountain stream at the Miya Valley. In downstream of the exit, water course was narrowed by sediment deposition. In the upstream reach, the width of water surface was extended since river channel blockade raised water level. Fukuda et al. (2012) confirmed the supply of the white-colored stones from upstream of Asahi Dam and recovery mechanism of riffles and pools by construction of the sediment bypass tunnel. However, a large amount of gray stones due to slope failures were supplied and deposited on sandbars, and water course was rectilinear after the flood.

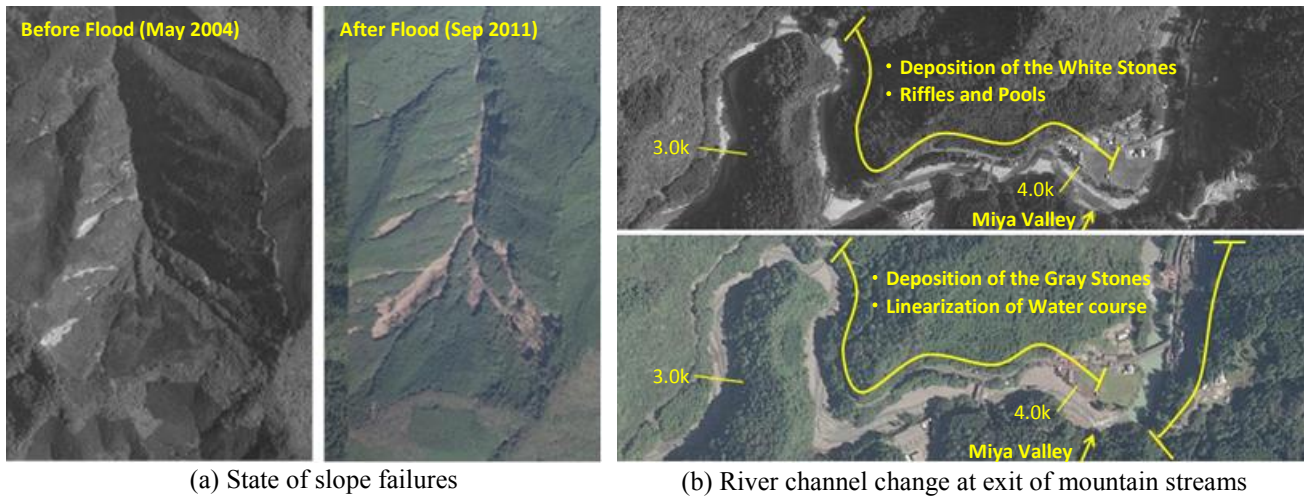


Figure 4. Comparison between aerial photographs before and after the flood.

Figure 5 shows the longitudinal distributions of the average and deepest elevations of the river bed observed before and after the flood. Large-scale slope failures were identified at the Miya Valley which met the Asahi River at about 4.0km point. The average bed elevation was raised about 1.5m and deepest bed elevation about 3.0m around the exit of the Miya Valley.

The volume of sediment deposition in the upstream of the sediment storage dam is about 48,000m<sup>3</sup>, in the Dam Reservoir is 299,800m<sup>3</sup>, and in the downstream of the Dam is 249,000m<sup>3</sup>. It is important to consider large-scale sediment inflow as an upstream boundary conditions of debris flows since the effect of the sediment inflow to the Asahi River from the Miya Valley is so large.

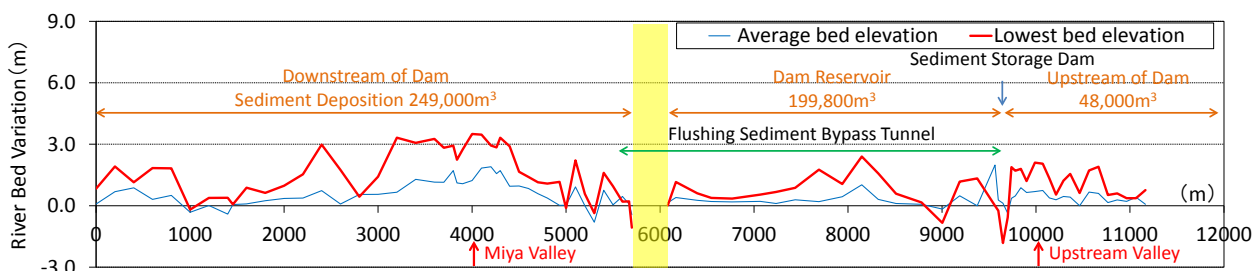


Figure 5. Average and lowest bed elevations and sediment deposition volumes.

## 3 ESTIMATION OF SEDIMENT INFLOW VOLUME

### 3.1 Estimation of the occurrence time by slope failures

Large-scale sediment supply due to slope failures and changes in river channel geometry appear in the temporal changes in water surface profiles. We estimated the occurrence time of slope failures from two-dimensional flood flow analysis using cross-sectional bed shapes observed before and after floods and comparison of observed and calculated water levels.

The analysis was performed from the junction with the Kumano River to 2.0km upstream of the entrance of the sediment bypass tunnel. The initial bed forms were given based on cross-sectional bed shapes measured before (2011) and after (2012) the flood. The numerical model was applied to the flood occurred in September 2011. Water level and discharge have been measured at observation points at upstream and downstream of Asahi Dam. In downstream observation point, water levels were not measured because the water gauge was damaged by sedimentation after the large amount of sediment inflow. The upstream boundary condition was given by observed discharge hydrographs at the upstream observation point. The downstream boundary condition was given by the uniform flow depth. The manning roughness coefficients was  $n=0.035$  so as to explain the observed water-level hydrographs in the observation points.

Figure 6 shows the comparison between observed and calculated water-level hydrographs and occurrence time of slope failures. In early stage, the calculated water levels using channel cross-section before the flood was similar to observed one in upstream observation point. And about 25 hours later, the calculated water levels using channel cross-section after the flood was in rather good agreements with observed one. On the other hand, in the downstream observation point, the calculated water levels using channel cross-section before the flood were similar to flood peak. And about 66 hours later, the calculated water levels using channel cross-section after the flood explained observed one. Since changes in geometrical condition of river channel appears in the observed water levels, it is assumed that the large sediment supply from the Miya Valley has been occurred at about 25 hours in upstream and about 66 hours in downstream observation point, respectively.

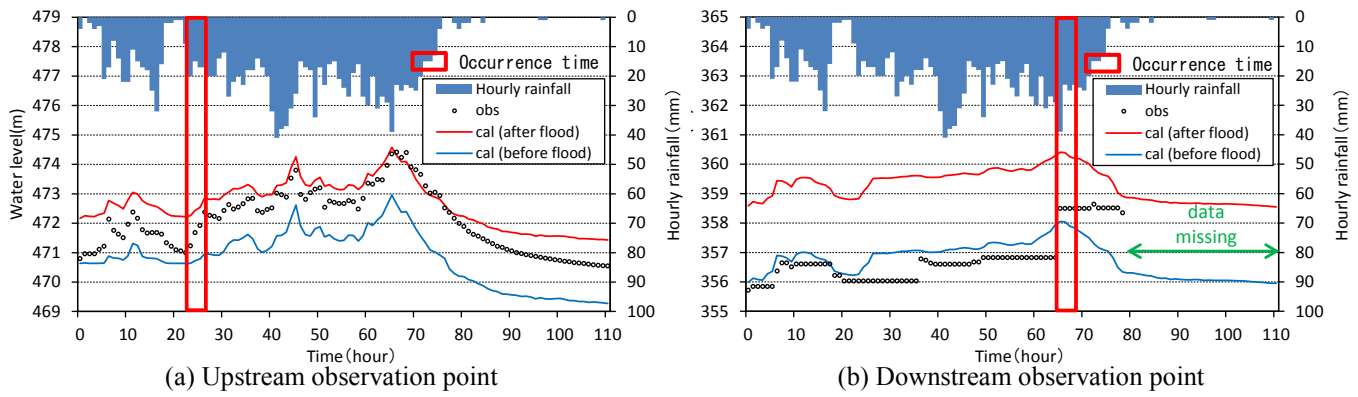


Figure 6. Occurrence time of slope failures predicted from observed and calculated water level hydrographs.

### 3.2 Estimation of the sediment inflow volume

#### 3.2.1 Sediment runoff analysis model due to slope failures

The volume of sediment runoff was calculated by the kinematic wave runoff model which simulated surface and subsurface runoff and the stability analysis assuming the slope of infinite length (Ichikawa (1999)). The equation of the kinematic wave runoff model is written as:

$$\frac{\partial q}{\partial x} + \frac{\partial h}{\partial t} = r \quad (1)$$

$$q = \begin{cases} ah & (h \leq d) \\ \alpha(h - d)^m + ah & (h > d) \end{cases} \quad (2)$$

Where,  $q$ : unit width discharge,  $h$ : water depth,  $d$ : subsurface layer thickness,  $r$ : rainfall intensity,  $a = k \sin \theta / \gamma$ ,  $k$ : coefficient of permeability,  $\gamma$ : effective porosity,  $\theta$ : slope gradient,  $\alpha = \sqrt{\sin \theta} / n$ ,  $m=5/3$ ,  $n$ : manning roughness coefficients.

The safety-factor is defined the ratio of the shear stress  $\tau$  (Eq.(3)) bringing slope failures to the resisting stress  $\tau_r$  (Eq.(4)) by assuming the slope of infinite length. In this study, we assume the slope failures are occurred when safety-factor become less than 1.0 after the occurrence time of slope failures predicted from observed and calculated water level hydrographs (see figure 6).

$$\tau = \{\gamma_{sat} \cdot H + \gamma_t \cdot (D - H)\} \cdot \sin \theta \cdot \cos \theta \quad (3)$$

$$\begin{aligned} \tau_r &= c + (\sigma - u) \cdot \tan \varphi \\ &= c + \{(\gamma_{sat} - \gamma_w) \cdot H + \gamma_t \cdot (D - H)\} \cos^2 \theta \cdot \tan \varphi \end{aligned} \quad (4)$$

Where,  $c$ : adhesive force,  $\sigma$ : vertical stress of soil,  $u$ : pore-water pressure of soil,  $\varphi$ : internal frictional angle of soil,  $\gamma_{sat}$ : saturated unit weight of soil,  $\gamma_w$ : unit weight of water,  $\gamma_t$ : wet unit weight of soil,  $D$ : subsurface layer thickness,  $H$ : subsurface layer water depth.

### 3.2.2 Sediment inflow analysis model due to debris flow

The sediment inflows from mountain stream to the river channel was simulated by using debris flow equations which corresponded to each regime such as stony debris flow, immature debris flow, and bed load (Takahashi (2001)). The debris flow was calculated by one dimensional bed variation Equation (5)-(7).

$$\frac{\partial h}{\partial t} + \frac{\partial q}{\partial x} = i \quad (5)$$

$$\frac{\partial h}{\partial t} + \beta \frac{\partial(Uq)}{\partial x} = g h \sin\theta - g h \frac{\partial(z_b + h)}{\partial x} \cos\theta - \frac{\tau_b}{\rho_t} \quad (6)$$

$$\frac{\partial(C_h)}{\partial t} + \frac{\partial(Cq)}{\partial x} = i C_* \quad (7)$$

Where,  $i$ : erosion and deposition velocity of the bed,  $\beta$ : momentum correction coefficient,  $U$ : cross-sectional average-flow velocity,  $g$ : acceleration of gravity,  $z_b$ : bed level,  $\tau_b$ : bed shear stress,  $\rho_t = \rho(1 - C) + \sigma C$ ,  $\rho$ : density of water,  $\sigma$ : density of soil,  $C$ : volume concentration of debris flow,  $C_*$ : volume concentration of sediment deposit.

The resistance laws in the river bed are given as follows:

For stony debris flow (when  $C \geq 0.4C_*$ )

$$\tau_b = \left(\frac{\sigma}{8}\right) \left\{ \left(\frac{C_*}{C}\right)^{1/3} - 1 \right\} \left(\frac{d}{h}\right)^2 U^2 \quad (8)$$

For immature debris flow (when  $0.01 < C < 0.4C_*$ )

$$\tau_b = \left(\frac{\rho_t}{0.49}\right) \left(\frac{d_L}{h}\right)^2 U^2 \quad (9)$$

For bed load (when  $C \leq 0.01$  or  $h/d \geq 30$ )

$$\tau_b = \frac{\rho g n^2}{h^{1/3}} U^2 \quad (10)$$

Where,  $d$ : representative grain size of soil particle,  $n$ : manning roughness coefficient.

The erosion and deposition velocity of the bed and equilibrium concentration are given as follows:

For erosion of the bed (when  $C < C_*$ )

$$i = \delta_e \frac{C_\infty - C}{C_* - C_\infty} \frac{q}{d} \quad (11)$$

For deposition of the bed (when  $C \geq C_*$ )

$$i = \delta_d \frac{C_\infty - C}{C_*} \frac{q}{h} \quad (12)$$

$$C_\infty = \frac{\rho \tan\theta_w}{(\sigma - \rho)(\tan\varphi - \tan\theta_w)} \quad (13)$$

Where,  $\delta_e$ : erosion velocity coefficient,  $\delta_d$ : deposition velocity coefficient,  $\theta_w$ : internal frictional angle.

### 3.2.3 Numerical analyse of slope failures and debris flows

In slope failure model, the slope unit data was created by 50m mesh based on 5.0m mesh data (Basic map information by Geographical Information Authority of Japan). Moreover, the slope direction and gradient were divided from the drainage paths in each mesh. The parameters of slope failure model are shown in table-1. Since the characteristics of soil such as adhesive force and an internal frictional angle were unknown, we set values used in other researches by slope failure model. The thickness of slope unit was assumed 0.6m in the Miya Valley and 0.2m in the Upstream Valley by the columnar section of soil in Mt. Shakagatake.

In debris flow model, longitudinal and cross-sectional shapes were made by the 5.0m mesh data. The analysis was performed 1.5km reach in the Miya Valley and 1.2km reach in the Upstream Valley. The longitudinal distance for the calculation was set about 50m-70m. The parameters of the debris flow model are shown in table 2. Since the characteristics of sediment inflow from mountain stream in the Asahi River basin were unknown, we set values of other researches used by debris flow model. Sediment supply due to slope failures was modeled assuming the process of temporal sedimentation and blockade in mountain stream.

Table 1. Parameter of slope failure model.

Thickness of slope unit (Miya Valley)	0.6m
"    (Upstream Valley)	0.2m
Equivalent roughness coefficient	0.035
Porosity	0.4
Coefficient of permeability	0.005m/s
Adhesive force	2.5kgN/m <sup>2</sup>
Internal frictional angle	20°

Table 2. Parameter of stony debris flow model.

Thickness of sediment deposit	3.0m
Density of coarse particles	2,650kg/m <sup>3</sup>
Density of water	1,000kg/m <sup>3</sup>
Volume concentration of the bed	0.65
Erosion velocity coefficient	0.0050
Deposition velocity coefficient	0.0003
Manning roughness coefficient	0.050

### 3.2.4 Result of analysis

Figure 7 shows the hourly rainfall and calculated sediment runoff volume by the slope failures. In the Miya Valley, slope failures were caused at the third peak of the rainfalls and the sediment runoff volume was estimated about 215,000m<sup>3</sup>. In the Upstream Valley, the sediment runoff volume was about 25,000m<sup>3</sup>.

Figure 8 shows calculated sediment inflow from the Miya Valley to the river channel, and its total volume. The total volume of the sediment inflow was estimated about 195,000m<sup>3</sup> in the Miya Valley and about 3,700m<sup>3</sup> in the Upstream Valley. In the Miya Valley, the total volume of sediment inflow was equivalent to about 78% of volume of the sediment deposition in the river channel at the down stream of the Dam ( 249,000m<sup>3</sup>, see Figure 5 ).

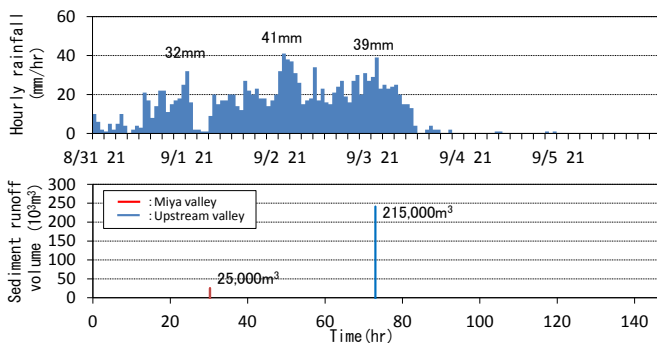


Figure 7. Observed hourly rainfall and calculated sediment runoff volume.

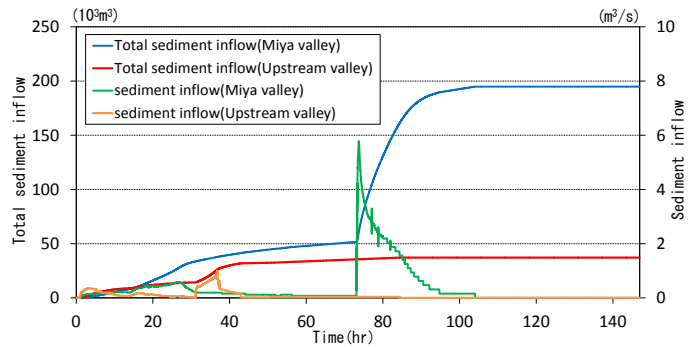


Figure 8. Calculated sediment inflow from mountain streams.

## 4 RIVER BED VARIATION ANALYSIS CONSIDERING LARGE-SCALE SEDIMENT INFLOW

### 4.1 Concept of the river bed variation analysis considering large-scale sediment inflow

We conducted two-dimensional river bed variation analysis in stony-bed river considering large-scale sediment inflow as boundary conditions. Figure 9 shows the concept of the process of aggradation by sediment inflow from mountain stream. Average height of each particle size  $\bar{Z}_{p,k}$  was estimated by using pick-up rate  $V_{p,k}$  and deposit rate  $V_{D,k}$  and each particle size function on the bed surface  $P_k$ . In order to consider the process of river bed aggradation and temporal river channel blockade, the volume of sediment inflow  $V_{in,k}$  was assumed to deposit with deposit rate  $V_{D,k}$  (Eq.(14)). The sediment deposition section was set in the remarkable section of sedimentation based on observed data indicated by the red frame in figure 11.

$$\frac{\partial \bar{Z}_{P,k}}{\partial t} = - \frac{\alpha_2 (V_{P,k} - (V_{D,k} + V_{in,k}))}{\alpha_3 P_k} \quad (14)$$

Where,  $\alpha_1, \alpha_2$ : 2-D and 3-D shape factors of the particles ( $=\pi/4, \pi/6$ ),  $k$ : each particle size.

The grain size distributions of the Asahi River and sediment inflow is shown in figure 10. The grain size distributions of sediment inflow were given by field survey in 2013. In the river channel, the grain size distributions surveyed by 2000 were used. Equilibrium sediment transport rate was assumed for the upstream boundary conditions.

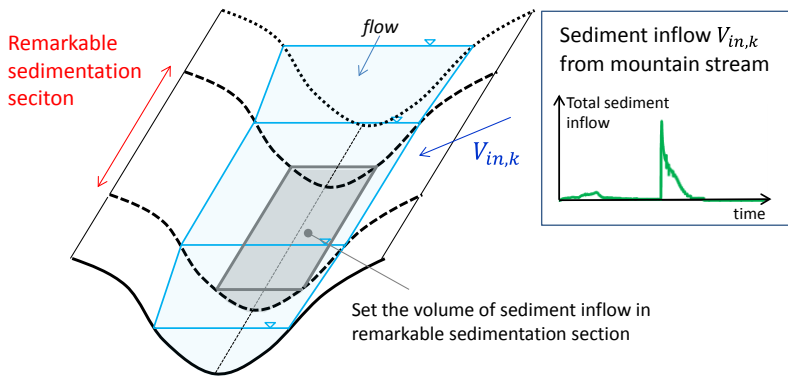


Figure 9. Concept of the river bed variation analysis considering large-scale sediment inflow.

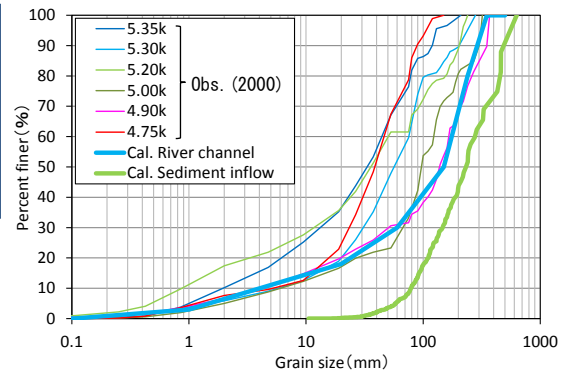


Figure 10. Grain size distributions used for analysis.

#### 4.2 Results and considerations

Figure 11 shows the comparison between the calculated and observed river bed variation contours before and after the flood. The height of the calculated sediment depositions was about 1.0m lower than the observed one through the area in the exit of the Miya Valley. In the upstream of the Dam, the height of calculated sediment deposition was similar to observed one at the exit of the Upstream Valley, but the height of calculated sediment deposition was lower than observed one near the entrance of sediment bypass tunnel. As shown below, this model cannot explain the extension of deposition area and process of sediment deposition since the large inertial force in sediment inflow has not considered, and thus cannot reproduce properly the height of the sediment deposition. However, calculated bed variations reproduce the sediment depositions of the observed data, especially the sediment depositions and temporal river channel blockade around the exit of the Miya Valley. Figure 12 shows the distribution of grain size D80. After the flood, larger size materials were transported in sediment deposition area due to sediment inflows.

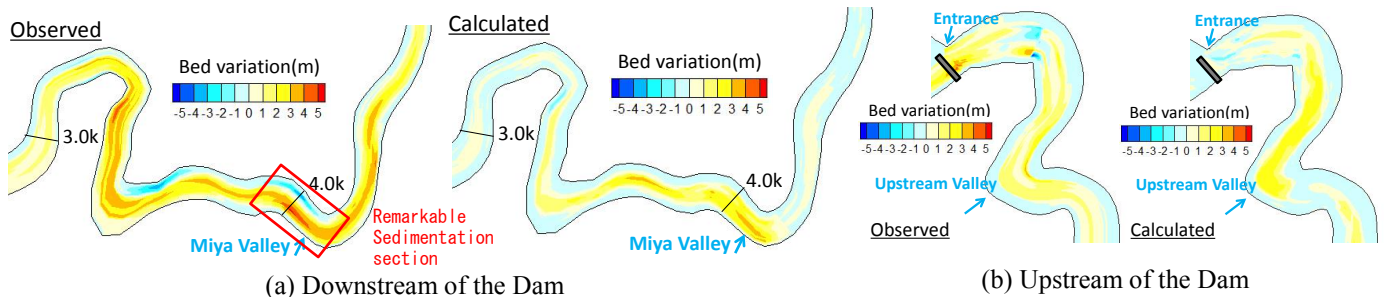


Figure 11. Comparison between calculated and observed river bed variation contour (After the flood).

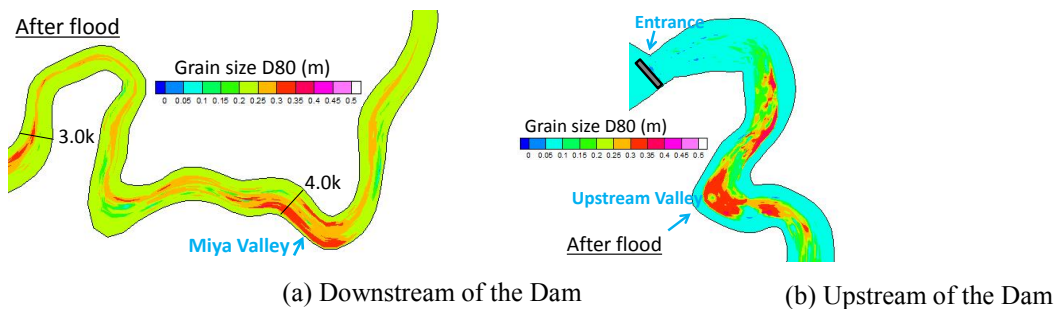


Figure 12. Distribution of grain size D80.

Figure 13 shows the calculated longitudinal peak water level. Flood marks were observed by field survey at the left-bank in downstream of the Miya Valley, and the calculated longitudinal peak water level repro-

duced observed one. We used the observed peak water level as a reference water level at downstream observation point, because the water gauge was not available by sedimentation.

The analysis gives overall explanation for the flood flows and the bed variations during 2011 flood considering large-scale sediment inflow from mountain stream.

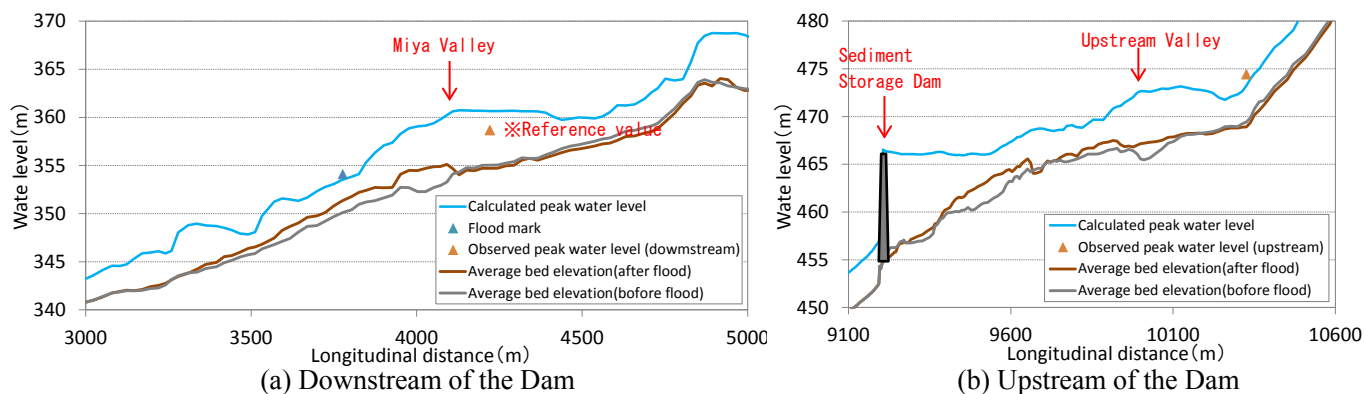


Figure 13. Calculated longitudinal peak water level.

## 5 CONCLUSION

In this paper, we clarified the sediment transports mechanism including the large sediment supply of the debris flows due to the slope failures in the Asahi River basin during the 2011 flood.

Main conclusions are drawn as follows.

1. Observed data showed that river channel characteristics (channel shapes, grain size distribution) remarkably changed by large-scale sediment inflow due to slope failures and debris flows.
2. The volume of sediment inflow was estimated by slope failure model and debris flow model. They were combined with two-dimensional flood flows and river bed variation analysis model to clarify the relationship between flood flows and river sediment transports accompanying the large amount of sediment supply.
3. It was shown that the analysis gave overall explanations for flood flows and bed variations during 2011 flood considering large-scale sediment inflow from mountain stream and that to consider the large-scale sediment inflow in river bed variation as boundary conditions was important to solve properly the problem treated in the paper.

## REFERENCES

- Fukuda, T., Yamashita, K., Osada, K. and Fukuoka, S. (2012): Study on Flushing Mechanism of Dam Reservoir Sedimentation and Recovery of Riffle-Pool in Downstream Reach by a Flushing Bypass Tunnel, International Symposium on DAMS FOR A CHANGING WORLD-Need for Knowledge Transfer across the Generations & the World, Kyoto, Japan.
- Osada, K. and Fukuoka, S. (2013): Two-dimensional riverbed variation analysis method focused on bed surface unevenness and mechanism of sediment transport in stony-bed rivers, THESIS 2013, Chatou, France.
- Bathurst, J. C. (2002): Physically-based erosion and sediment yield modelling: the SHETRAN concept, IHP-VI Technical Document in Hydrology, No.60, UNESCO, Paris, pp. 47-67.
- Hirasawa, R., Satofuka, Y., Mizuyama, T. and Tsutsumi, D. (2012): Development and Application of a Sediment Runoff from a Mountain Watershed Simulator (SERMOW-II), Journal of the Japan Society of Erosion Control Engineering, Vol. 64, No.5.
- Ichikawa, Y., Satoh, Y., Shiiba, M., Tachikawa, Y. and Takara K. (1999): Development of Water and Sediment Flow Model for a Mountains Area, Prev. Res. Inst., Kyoto University, 42 B-2, pp. 211-224.
- Takahashi, T., Inoue, M., Nakagawa, H. and Satofuka, Y. (2001): Prediction of Sedimentation Process In A Reservoir using a Sediment Runoff Modell, Annual Journal of Hydraulic Engineering, JSCE, Vol. 45, pp. 841-846.